

# Electronic and Functional Scope of Boronic Acid Derived Salicylidenehydrazone (BASHY) Complexes as Fluorescent Dyes

María M. Alcaide,<sup>†</sup> Fabio M. F. Santos,<sup>‡</sup> Vânia F. Pais,<sup>†</sup> Joana Inês Carvalho,<sup>‡</sup> Daniel Collado,<sup>§,||</sup> Ezequiel Pérez-Inestrosa,<sup>§,||</sup> Jesús F. Arteaga,<sup>†</sup> Francisco Boscá,<sup>⊥</sup> Pedro M. P. Gois,<sup>\*,‡</sup> and Uwe Pischel<sup>\*,†</sup>

<sup>†</sup>CIQSO – Center for Research in Sustainable Chemistry and Department of Chemistry, University of Huelva, Campus de El Carmen s/n, E-21071 Huelva, Spain

<sup>‡</sup>Research Institute for Medicines (iMed.Ulisboa), Faculty of Pharmacy, Universidade de Lisboa, 1600-276 Lisbon, Portugal

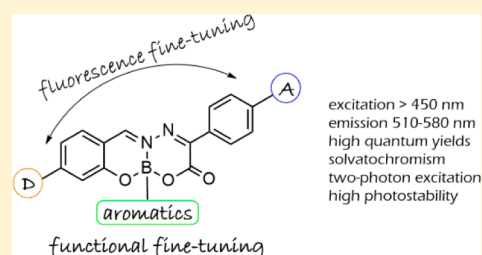
<sup>§</sup>Department of Organic Chemistry, University of Málaga, IBIMA, Campus Teatinos s/n, E-29071 Málaga, Spain

<sup>||</sup>Andalusian Center for Nanomedicine and Biotechnology – BIONAND, Parque Tecnológico de Andalucía, E-29590 Málaga, Spain

<sup>⊥</sup>Institute of Chemical Technology (CSIC-UPV), Polytechnical University of Valencia, Av. de los Naranjos s/n, E-46022 Valencia, Spain

## Supporting Information

**ABSTRACT:** A series of boronic acid derived salicylidenehydrazone (BASHY) complexes was prepared and photophysically characterized. The dye platform can be modified by (a) electronic tuning along the cyanine-type axis via modification of the donor–acceptor pair and (b) functional tuning via the boronic acid residue. On the one hand, approach (a) allows the control of photophysical parameters such as Stokes shift, emission color, and two-photon-absorption (2PA) cross section. The resulting dyes show emission light-up behavior in nonpolar media and are characterized by high fluorescence quantum yields (ca. 0.5–0.7) and brightness (ca. 35000–40000 M<sup>-1</sup> cm<sup>-1</sup>). Moreover, the 2PA cross sections reach values in the order of 200–300 GM. On the other hand, the variation of the dye structure through the boronic acid derived moiety (approach (b)) enables the functionalization of the BASHY platform for a broad spectrum of potential applications, ranging from biorelevant contexts to optoelectronic materials. Importantly, this functionalization is generally electronically orthogonal with respect to the dye's photophysical properties, which are only determined by the electronic structure of the cyanine-type backbone (approach (a)). Rare exceptions to this generalization are the presence of redox-active residues (such a triphenylamine or pyrene). Finally, the advantageous photophysics is complemented by a significant photostability.



## INTRODUCTION

The development of fluorescent dyes that correspond to the demands of optoelectronic or biomedical applications is an evergreen research topic at the intersection of synthetic chemistry and photosciences. There have been considerable efforts to improve archetypal fluorophore platforms such as fluoresceins,<sup>1–3</sup> rhodamines,<sup>1–4</sup> and Bodipy dyes<sup>2,5–13</sup> with respect to their photophysical performance, e.g., excitation with visible light, high emission quantum yields, and fluorescence at wavelengths larger than 500 nm. The applied strategies imply often the cumbersome redesign of the synthetic route to achieve modifications of the skeleton itself or its substitution pattern. Unfortunately, frequently the modification of functional aspects such as the introduction of a recognition motif or bio-orthogonal handles may also influence the electronic properties of the dye in an unwanted manner. It is therefore desirable to get hands on a platform where the same ligand system could give rise to fluorescent dyes with a large molecular diversity by means of a straightforward assembly reaction with a

variable component, without having to worry about unwanted modifications of the photophysical properties.

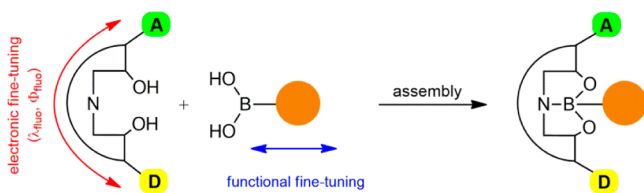
Boron(III) architectures, especially as tetracoordinated complexes, have enjoyed special attention for the design of fluorescent dyes,<sup>14–28</sup> not just limited to perhaps the most widely known case of the Bodipy dye family.<sup>2,5–13</sup> Building on the rich coordination chemistry of boronic acids,<sup>28–34</sup> we have recently developed a new fluorophore platform that can be accessed by a diversity-oriented synthetic strategy.<sup>35</sup> The dyes rely on the condensation of boronic acids (BAs) with a salicylidenehydrazone (SHY) ligand system, leading to BASHY dyes with intriguing photophysical properties and applications in bioimaging.<sup>35,36</sup> In this work we explore the photophysical scope of the dyes through the variation of both the *push–pull* charge-transfer character at the ligand backbone and the organic residue that is introduced with the boronic acid component. The orthogonal electronic and functional tuning

Received: March 13, 2017

Published: July 11, 2017

(see Scheme 1) and the ease of preparation, employing standard reactions with only minimal requirements for

### Scheme 1. Representation of the Structural Diversity of BASHY Dyes



additional purification, make BASHY dyes an interesting target. The structures of the investigated dyes (1–12) are shown in Chart 1.

The obtained dyes have very advantageous fluorescence properties including high emission quantum yield and brightness that are matched with pronounced solvatochromic effects and a good photochemical stability. The combination of these attributes is lacking for many dyes, for example, most often solvatochromic dyes are characterized by relatively low brightness and moderate photochemical stability.<sup>37</sup> In addition, we show herein for the first time that BASHY dyes are very efficient two-photon-absorbing chromophores with cross sections that are larger than those of traditional dyes used in multiphoton-excitation confocal fluorescence microscopy.<sup>38,39</sup>

## RESULTS AND DISCUSSION

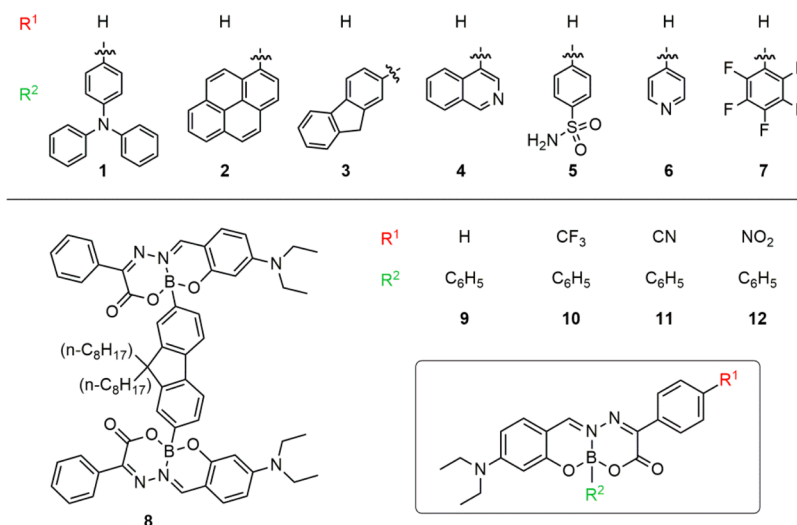
**Synthesis and Scope.** The synthesis of fluorescent BASHY dyes permits the flexible integration of a large variety of moieties in the last step of the reaction, consisting in the condensation of a boronic acid component with a non-fluorescent salicylidenehydrazone ligand (see Scheme 2).<sup>35</sup> This reaction is facile, straightforward, and often column chromatography is not required to obtain pure products in high yields (generally >96%). Attending the requirements on a *push–pull* charge-transfer architecture, we selected a ligand system (16a–d) with a strong electron-donating *N,N*-diethylamino group. The ligands are accessible from the

hydrazones 15a–d and 4-diethylaminosalicylaldehyde, following a described procedure (see Experimental Section).<sup>35</sup> The dyes were characterized for their purity and identity by <sup>1</sup>H, <sup>11</sup>B, and <sup>13</sup>C NMR spectroscopy as well as by elemental analysis or high-resolution mass spectrometry. The tetracoordinate nature of the dye was confirmed by <sup>11</sup>B NMR, yielding signals in the range of 3–6 ppm that are in accordance with sp<sup>3</sup> boron; see Experimental Section and Supporting Information for characterization data.

One of the aims of this study was to explore the functional diversity of the BASHY platform by means of variations of the boronic acid derived moiety (R<sup>2</sup> in Chart 1 and Scheme 2). The triphenylamine moiety, installed in dye 1, is a known strong electron donor. The opposite electronic situation is encountered for dye 7, containing a strongly electron-accepting pentafluorophenyl residue, also known for its importance as fluororous tag. Dye 5 features a phenylsulfonamide, a key structural motif of carbonic anhydrase inhibitors. Nitrogen-containing heterocyclic moieties such as the 4-isoquinolinyl (dye 4) or the 4-pyridyl (dye 6) were chosen for their possible implication in metal–ligand assemblies. Fluorene is a prominent chromophore in organic light-emitting diodes, motivating the preparation of the dyes 3 and 8. The integration of these diverse motifs generally does not alter the photo-physical properties of the electronically orthogonal boron salicylidenehydrazone backbone. Finally, the electronic demand of the distant phenyl substituent was varied through R<sup>1</sup> (R<sup>1</sup> = H, CF<sub>3</sub>, CN, NO<sub>2</sub>; see Chart 1). This provides a way to control the fluorescence properties by means of the degree of intramolecular charge transfer (ICT) along the cyanine-type backbone in 9–12.<sup>40</sup>

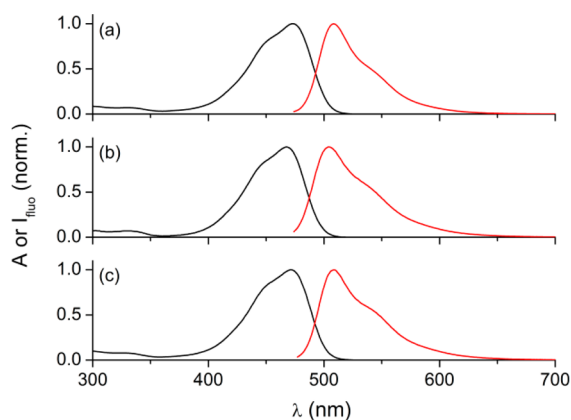
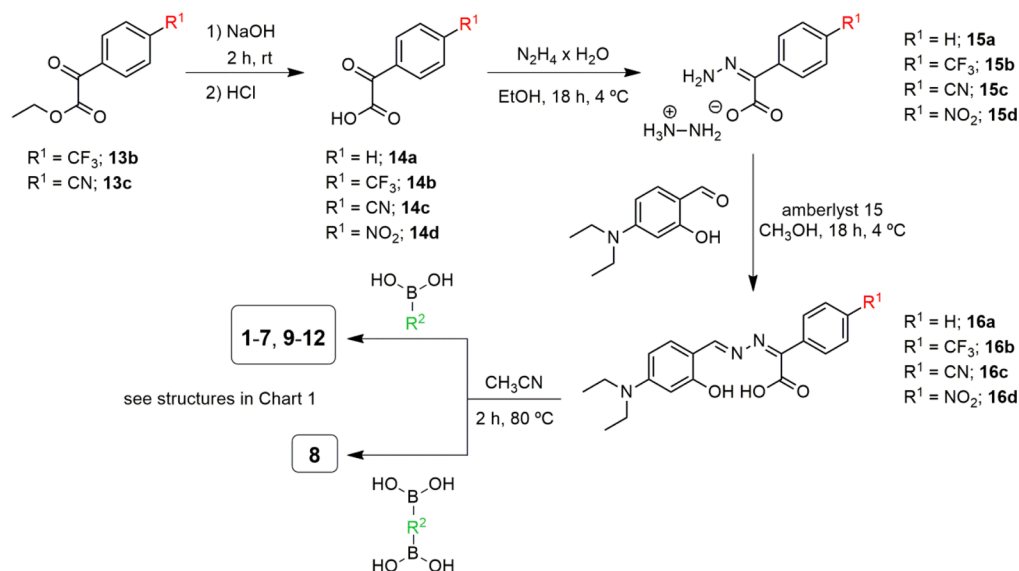
**Photophysical Properties of the Dyes 1–8.** The photophysical data of the dyes in air-equilibrated toluene and acetonitrile solutions are summarized in the Supporting Information, and example spectra in toluene are shown in the Figures 1 and 2. The dyes 3–8 feature very similar UV–vis absorption spectra with a maximum at about 465–475 nm and high molar absorption coefficients (generally 50,000–60,000 M<sup>-1</sup> cm<sup>-1</sup>; except for the dimeric BASHY 8, for which values as high as 121,000 M<sup>-1</sup> cm<sup>-1</sup> were observed) both in toluene and

Chart 1. Structures of the Dyes 1–12<sup>a</sup>



<sup>a</sup>Note that the formal charges in the BASHY structures have been omitted for the sake of clarity.

Scheme 2. Synthesis of the Dyes 1–12



**Figure 1.** UV-vis absorption (black) and fluorescence spectra (red) of the dyes **6** (a), **7** (b), and **9** (c) in air-equilibrated toluene. The fluorescence spectra were obtained by excitation at the maximum of the long-wavelength absorption band.

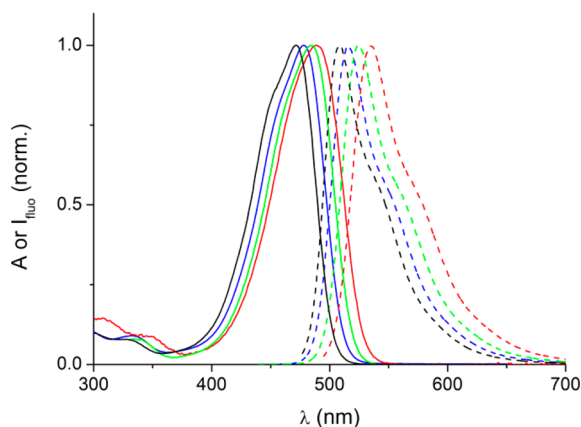


**Figure 2.** Normalized UV-vis absorption (solid lines) and fluorescence spectra (dashed lines) of dye **9** (black), **10** (blue), **11** (green), and **12** (red) in air-equilibrated toluene.

acetonitrile. The fluorescence emission maximum is located at 505–510 nm in toluene and at 540–545 nm in acetonitrile. The bathochromic shift of the emission, observed for the polar

acetonitrile, corroborates the at least partial involvement of ICT in the excited state, as has been suggested recently by quantum-chemical calculations of BASHY dyes.<sup>40</sup> Also the emission quantum yields ( $\Phi_{\text{fluo}}$ ) and lifetimes ( $\tau_{\text{fluo}}$ ) show parallel trends in dependence on the solvent. For toluene high quantum yields of about 0.5–0.7 were observed, while in acetonitrile, a drop to values of about 0.05–0.12 was noted. The fluorescence of BASHY dyes is not quenched by oxygen, as shown in quantum yield measurements with nitrogen-purged solutions of the representative dyes **2**, **5**, and **9** (quantum yields remain the same within an error margin of 10%). The fluorescence lifetimes are situated at ca. 2.4–3.0 ns in toluene and are significantly shorter in acetonitrile (ca. 0.3–0.5 ns). The proportionality between  $\Phi_{\text{fluo}}$  and  $\tau_{\text{fluo}}$  points to a rather solvent-independent radiative rate constant ( $k_r = \Phi_{\text{fluo}}/\tau_{\text{fluo}}$ ), being generally in the order of  $10^8 \text{ s}^{-1}$  for the herein investigated series (see Supporting Information). However, the nonradiative deactivation [ $k_{\text{nr}} = (1 - \Phi_{\text{fluo}})/\tau_{\text{fluo}}$ ] is by 1 order of magnitude faster in acetonitrile as compared to toluene (ca.  $10^9 \text{ s}^{-1}$  versus  $10^8 \text{ s}^{-1}$ ; see Supporting Information). This may be reasoned with the energy-gap law, predicting a faster  $S_1$ – $S_0$  deactivation for energetically lower lying excited singlet states. An alternative explanation could be a more efficient intersystem crossing to a close lying excited triplet state (see laser-flash photolysis study of dye **2** in Supporting Information). However, a recent theoretical study on BASHY complexes, including **9** and **12**, revealed that this is not a general photophysical pattern of these dyes.<sup>40</sup> These joint observations demonstrate that in general the electronic properties of the BA-derived aromatic moiety ( $R^2$ ; see Scheme 1) have only minor influence on the photophysical properties of the BASHY dye. Gratifyingly, this allows the orthogonal assembly of BASHY dyes, where the photophysical properties are practically only determined by the electronic properties of the boron salicylidenehydrazone backbone (see below for the dyes **9**–**12**). The invariability of the electronic structure of the BASHY backbone was confirmed by electrochemical measurements. The reduction of the BASHY core proceeded at peak potentials that are located for most of the dyes at ca.  $-1.1 \text{ V}$  (in dichloromethane); see Supporting Information.

The brightness ( $\epsilon \times \Phi_{\text{fluo}}$ ) of the dyes is especially pronounced in nonpolar media, reaching values of up to  $37,000 \text{ M}^{-1} \text{ cm}^{-1}$  (for dye **6**) or even  $76,000 \text{ M}^{-1} \text{ cm}^{-1}$  for the dimeric BASHY dye **8** in toluene. These values are comparable to or even larger than those of bright-emitting traditional dyes, such as fluoresceins, rhodamines, cyanines, boron dipyrromethene (Bodipy) dyes, or 7-nitrobenzoxadiazole (NBD) ICT dyes (see Supporting Information for a comparison of the photophysical properties of BASHY dyes with NBD or Bodipy).<sup>2</sup>

However, there are exceptions which are reflected in the observations that were made for the dyes **1** and **2**. These dyes show very low fluorescence quantum yields in toluene ( $\leq 0.02$ ) and are essentially nonfluorescent in acetonitrile. It is proposed that photoinduced electron transfer interferes, either in the excited singlet or triplet state. The involvement of an excited triplet state, populated via intersystem crossing, was shown for the example of dye **2** by performing nanosecond laser-flash photolysis experiments (see Supporting Information).

It is often observed that the photostability of solvatochromic dyes is considerably reduced in nonpolar solvents, implying triplet state formation and thereby photooxidations.<sup>37</sup> For this reason we tested this practically relevant aspect for some selected BASHY dyes in long-term irradiations of air-equilibrated toluene solutions with a 150 W Xe-lamp, exciting at  $>455 \text{ nm}$ . As judged from the changes in the UV-vis absorption spectrum, the dyes **1**, **3**, **9**, **11**, and **12** showed very minor decomposition (6% for **1**, 8% for **3**, and 3% for **9**, **11**, **12**) after 1 h of irradiation under comparable conditions. This very reduced photoreactivity is in accordance with the high fluorescence quantum yield in toluene. As an exception, dye **2** showed a pronounced tendency to photodecompose in air-equilibrated solution (61% after 1 h of irradiation); see Supporting Information.

**One- and Two-Photon Absorption Properties of the Dyes 9–12.** As discussed above, there is no bond-mediated electronic interaction between the BA-derived residue and the boron salicylidenehydrazone skeleton (except for dyes **1** and **2**). However, along the conformationally locked  $\pi$ -conjugated cyanine-type axis such communication is possible, especially when the extremes are substituted with an electron donor/acceptor (D/A) pair. This is manifested for the dyes **9–12**, featuring the  $\text{NEt}_2$  donor moiety and a distant phenyl ring with varying electron-accepting character. In line with this is the observation that incremented electron-acceptor strength of the phenyl *para*-substituent [Hammett constants  $\sigma_{\text{para}}$ : 0 (H), 0.54 ( $\text{CF}_3$ ), 0.66 (CN), 0.78 ( $\text{NO}_2$ )]<sup>41</sup> leads to increased bathochromic shifts of the absorption spectrum which is even more pronounced for the fluorescence spectrum (see Figure 2). Thus, on moving from dye **9** to dye **12** (containing the strongest electron-withdrawing substituent in the series), a bathochromic shift of the emission band by 27 nm was noted in toluene and even by 92 nm in acetonitrile. Again, this solvent dependence is in line with the proposed ICT character of the emissive state.<sup>40</sup> The quantum yields remain high for toluene throughout this dye series ( $\Phi_{\text{fluo}}$  ca. 0.55–0.65), but show a pronounced drop in polar solvents such as acetonitrile ( $\Phi_{\text{fluo}}$  ca. 0.05–0.08 for **9–11** and  $<0.01$  for **12**). This is in accordance with the observations made for the dyes **3–8** (see above). With the intention to showcase the solvatochromic character<sup>37</sup> of BASHY dyes, the fluorescence of **10–12** was investigated in a series of solvents (toluene, chloroform, tetrahydrofuran, ethyl acetate, acetone, acetonitrile, and dimethylformamide). All dyes

showed gradual bathochromic shifts of the emission spectrum and a decrease of the emission quantum yield upon increasing the solvent polarity (see Table 1 and Figure 3 as well as

**Table 1. Optical Properties of 10, 11, and 12 in Different Solvents**

	$\lambda_{\text{abs,max}}$ (nm)	$\lambda_{\text{fluo,max}}$ (nm)	$\Phi_{\text{fluo}}$
<b>Dye 10</b>			
toluene	478	516	0.65
chloroform	484	525	0.68
ethyl acetate	475	534	0.27
tetrahydrofuran	478	537	0.30
acetone	477	552	0.09
acetonitrile	476	559	0.05
dimethylformamide	481	566	0.08
<b>Dye 11</b>			
toluene	484	525	0.57
chloroform	492	537	0.56
ethyl acetate	481	546	0.25
tetrahydrofuran	483	549	0.28
acetone	483	567	0.09
acetonitrile	482	577	0.05
dimethylformamide	482	567	0.07
<b>Dye 12</b>			
toluene	489	535	0.55
chloroform	496	555	0.47
ethyl acetate	486	577	0.16
tetrahydrofuran	489	579	0.23
acetone	488	622	$<0.01$
acetonitrile	488	632	$<0.01$
dimethylformamide	494	636	$<0.01$

Supporting Information). The corresponding Lippert–Mataga plots<sup>42–44</sup> confirm the increasing *push–pull* character in the order  $10 < 11 < 12$  (see Supporting Information).

Recent time-dependent density functional theory calculations on BASHY dyes, including **9** and **12**, have shown that the  $\text{sp}^3$ -hybridized boron distorts the structure somewhat out of planarity with the dihedral angle that characterizes the relative

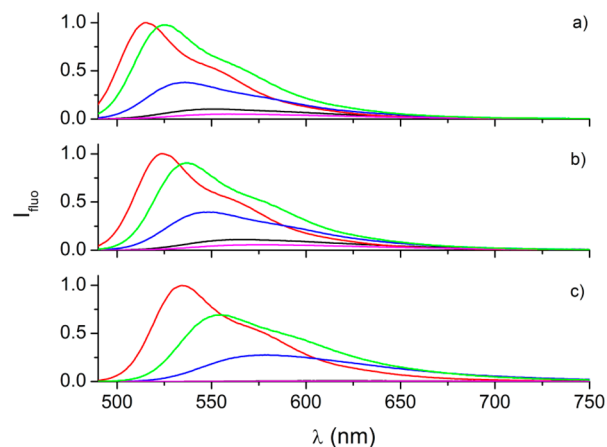


**Figure 3.** Fluorescence spectra of (a) **10**, (b) **11**, and (c) **12** in toluene (red), chloroform (green), tetrahydrofuran (blue), acetone (black), and acetonitrile (magenta). The spectra for each compound were recorded with optically matched solutions at identical excitation wavelength. Note that the spectra of **12** in acetone and acetonitrile coincide practically with the x-axis.



orientation of the diethylamino group and the keto group being ca. 30°. <sup>40</sup> Based on the combined results of the theoretical spectroscopy study, a mixed cyanine/charge-transfer character of the first singlet excited state of BASHY dyes was proposed. Naturally, the charge-transfer character depends on the electron-donor and -acceptor substitution, being in accordance with the herein presented experimental observations for the dyes 9–12.

Based on the D- $\pi$ -A architecture we expected the observation of significant two-photon-absorption (2PA) phenomena. <sup>22,45–49</sup> Hence, the 2PA spectra and cross sections ( $\sigma_2$ ) for 9–12 were measured; see Figure 4 and Table 2. Strong

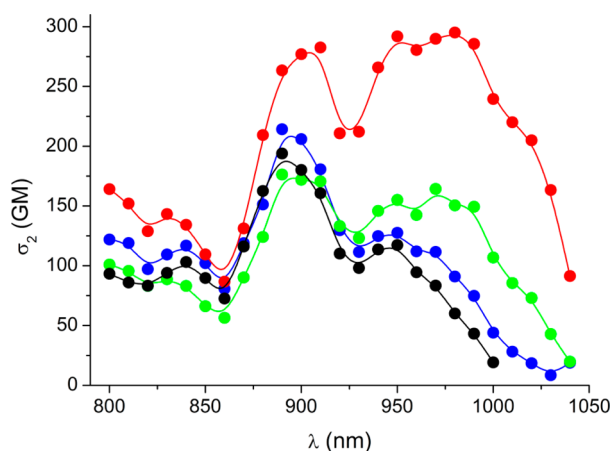


**Figure 4.** Two-photon absorption spectra of the dyes 9 (black), 10 (blue), 11 (green), and 12 (red) in air-equilibrated toluene.

**Table 2. Photophysical Data Related to Two-Photon Absorption of 9–12 in Toluene**

dye	two-photon process	
	$\lambda_{\text{two}}^{2\text{PE}}$ (nm)	$\sigma_2$ (GM)
9	508	194 (890 nm), 117 (950 nm)
10	518	214 (890 nm), 128 (950 nm)
11	528	176 (890 nm), 164 (970 nm)
12	537	283 (910 nm), 295 (980 nm)

2PA bands with maxima between ca. 900 and 1000 nm were observed. The 2PA cross sections reached values of almost 300 GM for dye 12 and ca. 200 GM for the other three dyes. These values are larger than observed for comparable *push-pull* dyes such as NBD dyes, <sup>50</sup> absorbing and emitting in the same spectral region as BASHY dyes (see Supporting Information). The two-photon excitation (2PE) led to the population of the lowest excited singlet state, resulting in the observation of the same fluorescence as observed in conventional one-photon spectroscopy (see Table 2 as well as Supporting Information).

## CONCLUSIONS

A series of BASHY dyes with varying electronic structure and functional aspects was prepared and photophysically characterized. Except for dyes that experience photoinduced electron-transfer phenomena, the electronic nature of BA-derived moieties has no influence on the UV-vis absorption and fluorescence properties. This is a direct consequence of the electronic isolation of these moieties from the boron salicylidenehydrazone backbone itself. This constitutes an advantage for the flexible molecular and functional diversifica-

tion of BASHY dyes without compromising their photophysical properties. The electronic fine-tuning along the cyanine-type backbone of the dyes opens possibilities for constructing D- $\pi$ -A wires with tailored emission properties as well as significant solvatochromic and two-photon-absorption behavior.

## EXPERIMENTAL SECTION

**Materials and General Methods.** The reactions were performed in flame-dried single-neck round-bottom flasks fitted with rubber septa and maintaining a positive pressure of argon, except for the synthesis of the dyes which were carried out in sealed tubes. Air- and moisture-sensitive liquids were transferred with the aid of a syringe or stainless steel cannules. All solvents were used as received, being of spectroscopic quality when employed for photophysical measurements.

Thin-layer chromatography was performed using silica gel 60 F<sub>254</sub> aluminum plates, visualized by UV light or revealed with an ethanolic solution of phosphomolybdic acid or bromocresol and heat. Column chromatography was performed using standard silica gel 60.

The NMR spectra ( $\delta$  values in ppm) were recorded on standard instrumentation, operated at 400 or 300 MHz (<sup>1</sup>H), 100 or 75 MHz (<sup>13</sup>C), and 128 MHz (<sup>11</sup>B), using CDCl<sub>3</sub> or (CD<sub>3</sub>)<sub>2</sub>SO as deuterated solvent. All coupling constants are expressed in Hz. High-resolution mass spectra were recorded on a triple quadrupole/linear ion trap mass spectrometer, using electrospray ionization (EI). The elemental composition was determined with a standard CHN analyzer. Infrared spectra of samples dispersed in KBr disks were recorded on a Fourier transform spectrometer with ceramic infrared light source and a deuterated L-alanine doped triglycine sulfate detector.

Electrochemical measurements were done in dichloromethane containing 0.1 M Bu<sub>4</sub>NPF<sub>6</sub> and at a scan rate of 100 mVs<sup>-1</sup>. The potentials are reported versus aqueous Ag/AgCl electrode and are not corrected for the junction potential. The E<sub>o</sub>' value for the ferrocenium/ferrocene couple used in this study was 0.46 V for dichloromethane solutions; glassy carbon electrode.

The employed boronic acid derivatives, hydrazine hydrate, 13b [ethyl oxo-(4-trifluoromethylphenyl)acetate], 13c (ethyl 4-cyanobenzoylformate), 14a (phenylglyoxylic acid), 14d (4-nitrophenylglyoxylic acid), 4-nitrosalicylaldehyde, and amberlyst 15 are commercially available in high purity and were used as received. The ligands 16a and 16d and the BASHY dyes 9 and 12 are known compounds and were available from an earlier project. <sup>55</sup>

**Preparation of the Ligand Precursors (16b and 16c). Phenylglyoxylic Acids 14.** The compounds 14b and 14c were prepared according to literature-known procedures. <sup>51,52</sup> In detail, the corresponding phenylglyoxylic ester (5.0 mmol) 13b or 13c was dissolved in 4.0 mL of an aqueous solution of NaOH (2.5 M) and stirred at room temperature for 2 h. Then the resulting mixture was acidified with 1 M HCl until pH < 7 and extracted with ethyl acetate (2 × 50 mL). The combined organic layers were dried over anhydrous magnesium sulfate, and then the volatiles were evaporated. The phenylglyoxylic acids were obtained as yellowish solids in excellent yields of 94% (14b) and 90% (14c), corresponding to 1.03 and 0.79 g, respectively. The crude was used immediately in the next reaction without further purification or characterization.

**Hydrazonophenylacetates 15.** Hydrazine hydrate (12.0 mmol) and the corresponding phenylglyoxylic acid 14b or 14c (4.0 mmol) were each dissolved in a separate portion of ethanol (2.0 mL). Then the two solutions were mixed in a round-bottom flask, and the reaction was continued for 18 h at 4 °C. After this time, the reaction mixture was filtered, and the obtained solid was washed twice with 700  $\mu$ L of cold ethanol. The hydrazonophenylacetates 15b and 15c were obtained in yields of 40% (422 mg) and 50% (442 mg), respectively, and used immediately in the next step without further purification or characterization.

**Salicylidenehydrazones 16.** Hydrazonophenylacetate 15b or 15c (2.0 mmol) was dissolved in 3.0 mL water, and then 22.0 mL methanol was added. This solution was slowly passed through a column packed with amberlyst 15 (3.0 mL of dry resin wetted with

methanol) into a round-bottom flask containing a solution of 4-diethylaminosalicylaldehyde in methanol (2.0 mmol in 3.0 mL). The resulting mixture was stirred for 2 h at room temperature and then left at 4 °C for further 18 h. Afterward the reaction mixture was filtered, and the obtained solid was washed with cold dichloromethane (3 × 3.0 mL) and cold methanol (2 × 1.0 mL). The ligands **16b** and **16c** were obtained as orange solids in 57% and 62% yield, respectively.

**Ligand 16b.** Orange solid, yield 57% (464 mg): <sup>1</sup>H NMR (300 MHz, (CD<sub>3</sub>)<sub>2</sub>SO) δ 8.77 (s, 1H), 7.96 (d, *J* = 8.7 Hz, 2H), 7.89 (d, *J* = 8.7 Hz, 2H), 7.38 (d, *J* = 9.0 Hz, 1H), 6.37 (dd, *J* = 9.0 and 2.1 Hz, 1H), 6.11 (d, *J* = 2.1 Hz, 1H), 3.41 (q, *J* = 6.9 Hz, 4H), 1.12 (t, *J* = 6.9 Hz, 6H) ppm; <sup>13</sup>C NMR (75 MHz, (CD<sub>3</sub>)<sub>2</sub>SO) δ 166.3, 165.3, 161.6, 157.3, 152.3, 135.5, 134.5, 127.5, 126.2, 126.14, 126.09, 126.0, 106.0, 104.8, 96.8, 44.1, 12.5 ppm; Elemental analysis calcd (%) for C<sub>20</sub>H<sub>20</sub>F<sub>3</sub>N<sub>3</sub>O<sub>3</sub> C 58.97, H 4.95, N 10.31. Found C 58.63, H 4.88, N 10.19.

**Ligand 16c.** Orange solid, yield 62% (452 mg): <sup>1</sup>H NMR (300 MHz, (CD<sub>3</sub>)<sub>2</sub>SO) δ 8.77 (s, 1H), 7.98 (d, *J* = 8.7 Hz, 2H), 7.90 (d, *J* = 8.7 Hz, 2H), 7.38 (d, *J* = 9.0 Hz, 1H), 6.38 (dd, *J* = 9.0 and 2.1 Hz, 1H), 6.11 (d, *J* = 2.1 Hz, 1H), 3.41 (q, *J* = 6.9 Hz, 4H), 1.12 (t, *J* = 6.9 Hz, 6H) ppm; <sup>13</sup>C NMR (75 MHz, (CD<sub>3</sub>)<sub>2</sub>SO): δ 166.1, 165.4, 161.7, 157.1, 152.4, 135.9, 134.5, 133.1, 127.4, 118.5, 113.0, 106.1, 104.8, 96.8, 44.1, 12.6 ppm; Elemental analysis calcd (%) for C<sub>20</sub>H<sub>20</sub>N<sub>4</sub>O<sub>3</sub> C 65.92, H 5.53, N 15.38. Found C 65.95, H 5.53, N 15.04.

#### General Procedure for the Preparation of the BASHY Dyes.

The synthesis of the dyes was performed by reaction of the corresponding ligand **16** and the appropriate boronic acid derivative.<sup>35</sup> For this purpose stoichiometric amounts of ligand **16** and the boronic acid (0.1 mmol in all cases, except for the synthesis of **8**, where 0.05 mmol of the boronic acid derivative were used) were dissolved in 1.0 mL acetonitrile and stirred at 80 °C for 2 h in a sealed tube. Then the volatiles were evaporated. In the case of the dyes **2**, **3**, **5–8**, **10**, and **11**, this procedure yielded high purity products in near quantitative yield without the need for further purification. Eventual trace impurities, that were observed in very few occasions, can be removed by washing the solid with a small amount of cold methanol. Exceptions from this very direct and straightforward procedure are the dyes **1** and **4** which required additional purification by preparative thin-layer chromatography for **1** using dichloromethane as eluent or flash column chromatography using *n*-hexane/CH<sub>2</sub>Cl<sub>2</sub> (1:9) for **4**.

**Dye 1.** Orange solid, yield 71% (42 mg): <sup>1</sup>H NMR (400 MHz, CDCl<sub>3</sub>) δ 8.17 (s, 1H), 7.94 (d, *J* = 7.9 Hz, 2H), 7.40–7.31 (m, 3H), 7.24–6.81 (m, 15H), 6.28 (d, *J* = 7.6 Hz, 1H), 6.16 (d, *J* = 1.6 Hz, 1H), 3.45–3.30 (m, 4H), 1.16 (t, *J* = 7.0 Hz, 6H) ppm; <sup>13</sup>C NMR (100 MHz, CDCl<sub>3</sub>) δ 161.7, 157.4, 156.0, 154.1, 153.6, 148.0, 147.5, 134.7, 132.8, 131.8, 131.0, 129.6, 129.3, 129.1, 128.3, 124.3, 123.3, 122.5, 107.7, 106.4, 98.7, 45.5, 12.9 ppm; <sup>11</sup>B NMR (128 MHz, CDCl<sub>3</sub>) δ 4.3 ppm; FTIR (KBr, cm<sup>-1</sup>) 2973, 2925, 2870, 2360, 1771, 1760, 1749, 1733, 1703, 1621, 1590, 1524, 1505, 1474, 1455, 1440, 1384, 1351, 1260, 1226, 1189, 1164, 1143, 1074, 1026, 971, 942, 828, 800, 789, 753, 715, 693, 420; HRMS (ESI) calcd for C<sub>37</sub>H<sub>34</sub>BN<sub>4</sub>O<sub>3</sub> [M + H]<sup>+</sup> 593.2718. Found 593.2707.

**Dye 2.** Orange solid, yield 99% (54 mg): mp 255–258 °C; <sup>1</sup>H NMR (300 MHz, CDCl<sub>3</sub>) δ 9.08 (d, *J* = 9.3 Hz, 1H), 8.54 (s, 1H), 8.16 (t, *J* = 7.8 Hz, 2H), 8.08 (d, *J* = 6.8 Hz, 1H), 7.97–7.91 (m, 6H), 7.65 (d, *J* = 7.6 Hz, 1H), 7.42–7.31 (m, 3H), 7.24 (d, *J* = 9.2 Hz, 1H), 6.29 (dd, *J* = 9.2 and 2.4 Hz, 1H), 6.09 (d, *J* = 2.1 Hz, 1H), 3.42–3.25 (m, 4H), 1.13 (t, *J* = 7.1 Hz, 6H) ppm; <sup>13</sup>C NMR (75 MHz, CDCl<sub>3</sub>) δ 161.6, 157.3, 155.7, 154.0, 153.7, 134.6, 134.3, 132.7, 131.4, 131.2, 130.9, 129.6, 129.3, 129.1, 128.3, 127.5, 127.1, 126.5, 125.6, 125.3, 125.2, 124.7, 124.3, 123.8, 108.0, 106.8, 98.8, 45.3, 12.7 ppm; <sup>11</sup>B NMR (128 MHz, CDCl<sub>3</sub>) δ 6.1 ppm; FTIR (KBr, cm<sup>-1</sup>) 2975, 2927, 2870, 2360, 1771, 1760, 1749, 1733, 1703, 1621, 1590, 1524, 1506, 1473, 1455, 1440, 1396, 1351, 1259, 1224, 1188, 1166, 1145, 1075, 1025, 974, 940, 829, 801, 793, 755, 714, 691, 420; Elemental analysis calcd (%) for C<sub>35</sub>H<sub>28</sub>BN<sub>3</sub>O<sub>3</sub> C 76.51, H 5.14, N 7.65. Found C 76.21, H 5.07, N 7.60.

**Dye 3.** Orange solid, yield 96% (49 mg): mp 235–238 °C; <sup>1</sup>H NMR (400 MHz, CDCl<sub>3</sub>) δ 8.34 (s, 1H), 7.99 (d, *J* = 7.0 Hz, 2H), 7.69 (d, *J* = 7.6 Hz, 1H), 7.63 (d, *J* = 7.7 Hz, 1H), 7.59 (s, 1H), 7.48–

7.37 (m, 5H), 7.31–7.20 (m, 3H), 6.38 (d, *J* = 8.9 Hz, 1H), 6.23 (s, 1H), 3.79 (s, 2H), 3.51–3.40 (m, 4H), 1.24 (t, *J* = 6.9 Hz, 6H) ppm; <sup>13</sup>C NMR (100 MHz, CDCl<sub>3</sub>) δ 161.7, 157.4, 156.0, 154.3, 153.7, 143.5, 142.7, 142.1, 141.5, 134.7, 132.8, 131.0, 129.6, 129.4, 128.3, 127.5, 126.6, 126.4, 125.0, 119.8, 119.2, 107.8, 106.5, 98.9, 45.5, 37.0, 12.9 ppm; <sup>11</sup>B NMR (128 MHz, CDCl<sub>3</sub>) δ 4.1 ppm; FTIR (KBr, cm<sup>-1</sup>) 2974, 2927, 2870, 2360, 1771, 1760, 1749, 1733, 1703, 1623, 1591, 1526, 1505, 1472, 1455, 1440, 1383, 1352, 1260, 1226, 1210, 1189, 1166, 1146, 1077, 1025, 976, 947, 918, 828, 800, 768, 712, 691, 419; HRMS (ESI) calcd for C<sub>32</sub>H<sub>29</sub>BN<sub>3</sub>O<sub>3</sub> [M + H]<sup>+</sup> 514.2296. Found 514.2290.

**Dye 4.** Orange solid, yield 75% (36 mg): <sup>1</sup>H NMR (400 MHz, CDCl<sub>3</sub>) δ 9.06 (s, 1H) 8.74 (d, *J* = 8.2 Hz, 1H), 8.47 (s, 1H), 8.08 (s, 1H), 7.97 (d, *J* = 8.8 Hz, 2H), 7.88 (d, *J* = 8.0 Hz, 1H), 7.75 (dt, *J* = 7.0 and 1.3 Hz, 1H), 7.56 (t, *J* = 7.0 Hz, 1H), 7.44–7.34 (m, 3H), 7.25 (d, *J* = 8.8 Hz, 1H), 6.34 (dd, *J* = 9.2 and 2.3 Hz, 1H), 6.07 (d, *J* = 2.2 Hz, 1H), 3.46–3.33 (m, 4H), 1.18 (t, *J* = 7.1 Hz, 6H) ppm; <sup>13</sup>C NMR (100 MHz, CDCl<sub>3</sub>) δ 161.4, 157.5, 155.5, 154.1, 153.4, 152.9, 144.8, 138.7, 134.9, 132.5, 131.1, 130.0, 129.7, 128.7, 128.3, 128.1, 126.6, 108.2, 106.8, 98.7, 45.4, 12.8; <sup>11</sup>B NMR (128 MHz, CDCl<sub>3</sub>) δ 5.5 ppm; FTIR (KBr, cm<sup>-1</sup>) 2973, 2924, 2870, 2360, 1771, 1760, 1749, 1733, 1622, 1592, 1526, 1504, 1475, 1455, 1441, 1383, 1350, 1261, 1223, 1189, 1166, 1146, 1077, 1054, 1025, 977, 826, 799, 782, 754, 714, 691, 420; HRMS (ESI) calcd for C<sub>28</sub>H<sub>26</sub>BN<sub>4</sub>O<sub>3</sub> [M + H]<sup>+</sup> 477.2092. Found 477.2089.

**Dye 5.** Orange solid, yield 98% (49 mg): <sup>1</sup>H NMR (400 MHz, CDCl<sub>3</sub>) δ 8.34 (s, 1H), 7.97 (d, *J* = 8.5 Hz, 2H), 7.73 (d, *J* = 8.4 Hz, 2H), 7.51 (d, *J* = 8.3 Hz, 2H), 7.47–7.37 (m, 3H), 7.24 (d, *J* = 9 Hz, 1H), 6.40 (dd, *J* = 9.1 and 2.4 Hz, 1H), 6.20 (s, 1H), 4.68 (s, 2H), 3.52–3.42 (m, 4H), 1.25 (t, *J* = 7.1 Hz, 6H) ppm; <sup>13</sup>C NMR (100 MHz, CDCl<sub>3</sub>) δ 161.4, 157.7, 155.5, 153.9, 153.7, 141.0, 134.8, 132.5, 131.6, 131.2, 129.6, 128.4, 125.6, 108.3, 106.5, 98.8, 45.6, 12.9 ppm; <sup>11</sup>B NMR (128 MHz, (CD<sub>3</sub>)<sub>2</sub>SO) δ -0.2 ppm; FTIR (KBr, cm<sup>-1</sup>) 2975, 2929, 2870, 2360, 1771, 1760, 1749, 1733, 1705, 1621, 1589, 1530, 1503, 1473, 1456, 1443, 1385, 1348, 1261, 1223, 1187, 1165, 1144, 1075, 1025, 975, 943, 828, 802, 759, 724, 713, 690, 420; HRMS (ESI) calcd for C<sub>25</sub>H<sub>25</sub>BN<sub>4</sub>O<sub>3</sub>NaS [M + Na]<sup>+</sup> 527.1531. Found 527.1523.

**Dye 6.** Orange solid, yield 99% (42 mg): mp 246–248 °C; <sup>1</sup>H NMR (300 MHz, CDCl<sub>3</sub>) δ 8.42 (d, *J* = 5.7 Hz, 2H), 8.32 (s, 1H), 7.98 (d, *J* = 6.9 Hz, 2H), 7.46–7.38 (m, 3H), 7.29–7.21 (m, 3H), 6.40 (dd, *J* = 9.3 and 2.0 Hz, 1H), 6.21 (d, *J* = 2.0 Hz, 1H), 3.54–3.40 (m, 4H), 1.26 (t, *J* = 6.9 Hz, 6H) ppm; <sup>13</sup>C NMR (75 MHz, CDCl<sub>3</sub>) δ 161.3, 157.7, 155.4, 153.8, 153.7, 148.4, 134.9, 132.4, 131.2, 129.5, 128.4, 126.1, 108.3, 106.4, 98.7, 45.6, 12.8 ppm; <sup>11</sup>B NMR (128 MHz, CDCl<sub>3</sub>) δ 3.5 ppm; FTIR (KBr, cm<sup>-1</sup>) 2973, 2933, 2870, 2360, 1771, 1760, 1749, 1733, 1712, 1626, 1592, 1527, 1506, 1472, 1456, 1441, 1386, 1353, 1263, 1220, 1187, 1170, 1145, 1079, 826, 798, 754, 714, 691, 420; Elemental analysis calcd (%) for C<sub>24</sub>H<sub>23</sub>BN<sub>4</sub>O<sub>3</sub> C 67.62, H 5.44, N 13.14. Found C 67.17, H 5.38, N 12.85.

**Dye 7.** Orange solid, yield 96% (49 mg): mp 235–237 °C; <sup>1</sup>H NMR (400 MHz, CDCl<sub>3</sub>) δ 8.24 (s, 1H), 8.02 (d, *J* = 7.2 Hz, 2H), 7.49–7.41 (m, 3H), 7.28 (s, 1H), 6.44 (d, *J* = 9.0 Hz, 1H), 6.21 (s, 1H), 3.54–3.43 (m, 4H), 1.27 (t, *J* = 7.0 Hz, 6H) ppm; <sup>13</sup>C NMR (100 MHz, CDCl<sub>3</sub>) δ 160.9, 157.7, 155.1, 154.7, 153.4, 134.7, 132.2, 131.3, 129.6, 128.5, 108.4, 106.4, 98.5, 45.6, 12.9 ppm; <sup>11</sup>B NMR (128 MHz, CDCl<sub>3</sub>) δ 2.2 ppm; FTIR (KBr, cm<sup>-1</sup>) 2979, 2932, 2875, 2360, 1771, 1760, 1749, 1733, 1714, 1625, 1594, 1527, 1508, 1458, 1384, 1353, 1289, 1262, 1220, 1189, 1168, 1147, 1025, 969, 927, 829, 801, 759, 745, 715, 692, 420; HRMS (ESI) calcd for C<sub>25</sub>H<sub>19</sub>BF<sub>3</sub>N<sub>3</sub>O<sub>3</sub>Na [M + Na]<sup>+</sup> 538.1332. Found 538.1331.

**Dye 8.** Orange solid, yield 99% (107 mg): <sup>1</sup>H NMR (300 MHz, CDCl<sub>3</sub>) δ 8.24 (s, 2H), 7.94 (d, *J* = 8.2 Hz, 4H), 7.41–7.18 (m, 14H), 6.35 (dd, *J* = 9.1 and 2.2 Hz, 2H), 6.24 (d, *J* = 2.0 Hz, 2H), 3.47–3.39 (m, 8H), 1.80–1.64 (m, 4H), 1.22 (t, *J* = 7.0 Hz, 12H), 1.17–0.23 (m, 30H) ppm; <sup>13</sup>C NMR (75 MHz, CDCl<sub>3</sub>) δ 161.8, 157.2, 156.2, 154.5, 153.5, 150.0, 141.1, 134.6, 132.7, 130.9, 129.4, 129.1, 128.3, 125.4, 118.9, 107.7, 106.4, 98.8, 54.7, 45.5, 40.3, 31.9, 30.3, 29.5, 29.4, 24.0, 22.8, 14.3, 12.8 ppm; <sup>11</sup>B NMR (128 MHz, CDCl<sub>3</sub>) δ 4.2 ppm; FTIR (KBr, cm<sup>-1</sup>) 2925, 2851, 2870, 1705, 1622, 1592, 1526, 1502, 1472,

1441, 1383, 1350, 1259, 1188, 1164, 1144, 1075, 1024, 971, 944, 923, 826, 801, 787, 753, 713, 691, 429; Elemental analysis calcd (%) for  $C_{67}H_{78}B_2N_6O_6$  C 74.17, H 7.25, N 7.75. Found C 73.72, H 7.42, N 7.50.

**Dye 10.** Red solid, yield 99% (49 mg): mp 228–230 °C;  $^1H$  NMR (300 MHz,  $CDCl_3$ )  $\delta$  8.30 (s, 1H), 8.12 (d,  $J$  = 8.1 Hz, 2H), 7.64 (d,  $J$  = 8.1 Hz, 2H), 7.39–7.36 (m, 2H), 7.25–7.19 (m, 4H), 6.39 (dd,  $J$  = 9.0 and 2.1 Hz, 1H), 6.20 (d,  $J$  = 2.1 Hz, 1H), 3.53–3.39 (m, 4H), 1.24 (t,  $J$  = 7.2 Hz, 6H) ppm;  $^{13}C$  NMR (75 MHz,  $CDCl_3$ )  $\delta$  161.9, 157.8, 155.7, 153.9, 152.1, 136.2, 134.9, 132.4, 132.0, 130.8, 129.9, 128.1, 127.8, 125.8, 125.2 (q,  $CF_3$ ), 108.3, 106.8, 98.8, 45.6, 12.9 ppm;  $^{11}B$  NMR (128 MHz,  $CDCl_3$ )  $\delta$  4.2 ppm; FTIR (KBr,  $cm^{-1}$ ) 2981, 2931, 2870, 2360, 2330, 1771, 1760, 1749, 1733, 1699, 1623, 1590, 1527, 1504, 1475, 1455, 1440, 1407, 1382, 1354, 1322, 1262, 1227, 1188, 1169, 1149, 1129, 1070, 1018, 977, 944, 853, 843, 822, 795, 714, 699, 420; Elemental analysis calcd (%) for  $C_{26}H_{23}BF_3N_3O_3$  C 63.31, H 4.70, N 8.52. Found C 63.72, H 4.87, N 8.47.

**Dye 11.** Red solid, yield 99% (45 mg): mp 287–289 °C;  $^1H$  NMR (300 MHz,  $CDCl_3$ )  $\delta$  8.29 (s, 1H), 8.13 (d,  $J$  = 9.0 Hz, 2H), 7.66 (d,  $J$  = 9.0 Hz, 2H), 7.37–7.34 (m, 2H), 7.24–7.19 (m, 4H), 6.40 (dd,  $J$  = 9.0 and 2.1 Hz, 1H), 6.20 (d,  $J$  = 2.1 Hz, 1H), 3.52–3.43 (m, 4H), 1.25 (t,  $J$  = 7.2 Hz, 6H) ppm;  $^{13}C$  NMR (75 MHz,  $CDCl_3$ )  $\delta$  162.0, 157.9, 155.5, 153.8, 151.1, 137.0, 135.1, 131.9, 130.8, 130.0, 128.1, 127.8, 118.6, 113.8, 108.5, 107.0, 98.7, 45.7, 12.9 ppm;  $^{11}B$  NMR (128 MHz,  $CDCl_3$ )  $\delta$  4.2 ppm; FTIR (KBr,  $cm^{-1}$ ) 2983, 2931, 2870, 2360, 2227, 1771, 1760, 1749, 1733, 1703, 1624, 1588, 1525, 1506, 1472, 1434, 1379, 1263, 1224, 1188, 1166, 1148, 1114, 1096, 1077, 1020, 974, 944, 823, 420; Elemental analysis calcd (%) for  $C_{26}H_{23}BN_4O_3$  C 69.35, H 5.22, N 12.21. Found C 69.43, H 5.22, N 12.21.

**Photophysical Measurements.** The photophysical measurements were performed with air-equilibrated solutions at room temperature, using quartz cuvettes (1 cm optical path length), except otherwise indicated. The UV–vis absorption spectra were obtained with a standard spectrophotometer. The fluorescence spectra were recorded with a fluorimeter equipped with a xenon flash-lamp as light source and corrected for the spectral sensitivity of the photomultiplier detector. The authenticity of the emission was confirmed by recording excitation spectra, monitoring the emission maximum. In all cases the excitation and absorption spectra matched each other. The fluorescence quantum yields were measured with 4-amino-*N*-propyl-1,8-naphthalimide ( $\Phi_{flu} = 0.48$  in acetonitrile)<sup>35</sup> as reference and corrected for refractive index differences of the used solvents. The lifetime measurements were done with the time-correlated single-photon-counting technique. For this purpose a picosecond pulsed diode laser ( $\lambda = 442$  nm, pulse width fwhm 78.3 ps) was used as excitation source. The detector was a multichannel photomultiplier, and the time response of the system was <50 ps.

The two-photon cross section ( $\sigma_2$ ) was determined by using the two-photon-induced fluorescence method with femtosecond pulsed excitation.<sup>53,54</sup> The compounds **9**, **10**, **11**, or **12** were dissolved in toluene (50.0  $\mu$ M), and the two-photon-induced fluorescence intensity was measured at 800–1040 nm, using rhodamine B (56.0  $\mu$ M in MeOH) as reference<sup>39</sup> and assuming that the fluorescence quantum yield remains the same regardless whether two-photon or one-photon excitation is used.<sup>55</sup>

## ASSOCIATED CONTENT

### Supporting Information

The Supporting Information is available free of charge on the ACS Publications website at DOI: 10.1021/acs.joc.7b00601.

Copies of  $^1H$ ,  $^{11}B$ , and  $^{13}C$  NMR spectra, FTIR spectra, additional photophysical data and electrochemical data (PDF)

## AUTHOR INFORMATION

### Corresponding Authors

\*E-mail: uwe.pischel@diq.uhu.es.

\*E-mail: pedrogois@ff.ulisboa.pt.

## ORCID

Joana Inês Carvalho: 0000-0002-9848-0203

Jesús F. Arteaga: 0000-0001-8153-6621

Uwe Pischel: 0000-0001-8893-9829

## Notes

The authors declare no competing financial interest.

## ACKNOWLEDGMENTS

The financial support by the Spanish MINECO (grants CTQ2014-54729-C2-1-P, CTQ2014-54729-C2-2-P, CTQ2013-41339-P, and CTQ2015-71896-REDT), the Junta de Andalucía (grant P12-FQM-2140), and Portuguese FCT (grants SFRH/BD/94779/2013, PTDC/REQ-QOR/1434/2014, iMed.Ulisboa grant UID/DTP/04138/2013) is gratefully acknowledged.

## REFERENCES

- Grimm, J. B.; Sung, A. J.; Legant, W. R.; Hulamm, P.; Matlosz, S. M.; Betzig, E.; Lavis, L. D. *ACS Chem. Biol.* **2013**, *8*, 1303–1310.
- Lavis, L. D.; Raines, R. T. *ACS Chem. Biol.* **2014**, *9*, 855–866.
- Kushida, Y.; Nagano, T.; Hanaoka, K. *Analyst* **2015**, *140*, 685–695.
- Beija, M.; Afonso, C. A. M.; Martinho, J. M. G. *Chem. Soc. Rev.* **2009**, *38*, 2410–2433.
- Loudet, A.; Burgess, K. *Chem. Rev.* **2007**, *107*, 4891–4932.
- Ulrich, G.; Ziessel, R.; Harriman, A. *Angew. Chem., Int. Ed.* **2008**, *47*, 1184–1201.
- Bozdemir, O. A.; Guliyev, R.; Buyukcaker, O.; Selcuk, S.; Kolemen, S.; Gulseren, G.; Nalbantoglu, T.; Boyaci, H.; Akkaya, E. U. *J. Am. Chem. Soc.* **2010**, *132*, 8029–8036.
- Boens, N.; Leen, V.; Dehaen, W. *Chem. Soc. Rev.* **2012**, *41*, 1130–1172.
- Niu, S.-l.; Massif, C.; Ulrich, G.; Renard, P.-Y.; Romieu, A.; Ziessel, R. *Chem. - Eur. J.* **2012**, *18*, 7229–7242.
- Kamkaew, A.; Lim, S. H.; Lee, H. B.; Kiew, L. V.; Chung, L. Y.; Burgess, K. *Chem. Soc. Rev.* **2013**, *42*, 77–88.
- Lu, H.; Mack, J.; Yang, Y.; Shen, Z. *Chem. Soc. Rev.* **2014**, *43*, 4778–4823.
- Kolemen, S.; Işık, M.; Kim, G. M.; Kim, D.; Geng, H.; Buyuktemiz, M.; Karatas, T.; Zhang, X.-F.; Dede, Y.; Yoon, J.; Akkaya, E. U. *Angew. Chem., Int. Ed.* **2015**, *54*, 5340–5344.
- Kowada, T.; Maeda, H.; Kikuchi, K. *Chem. Soc. Rev.* **2015**, *44*, 4953–4972.
- Liddle, B. J.; Silva, R. M.; Morin, T. J.; Macedo, F. P.; Shukla, R.; Lindeman, S. V.; Gardinier, J. R. *J. Org. Chem.* **2007**, *72*, S637–S646.
- Amarne, H.; Baik, C.; Murphy, S. K.; Wang, S. *Chem. - Eur. J.* **2010**, *16*, 4750–4761.
- Rao, Y.-L.; Wang, S. *Inorg. Chem.* **2011**, *50*, 12263–12274.
- Frath, D.; Poirel, A.; Ulrich, G.; De Nicola, A.; Ziessel, R. *Chem. Commun.* **2013**, *49*, 4908–4910.
- Frath, D.; Massue, J.; Ulrich, G.; Ziessel, R. *Angew. Chem., Int. Ed.* **2014**, *53*, 2290–2310.
- Yu, C.; Jiao, L.; Zhang, P.; Feng, Z.; Cheng, C.; Wei, Y.; Mu, X.; Hao, E. *Org. Lett.* **2014**, *16*, 3048–3051.
- Pais, V. F.; Lassaletta, J. M.; Fernández, R.; El-Sheshtawy, H. S.; Ros, A.; Pischel, U. *Chem. - Eur. J.* **2014**, *20*, 7638–7645.
- Tamgho, I.-S.; Hasheminasab, A.; Engle, J. T.; Nemykin, V. N.; Ziegler, C. J. *J. Am. Chem. Soc.* **2014**, *136*, S623–S626.
- Pais, V. F.; Alcaide, M. M.; Rodríguez-López, R.; Collado, D.; Nájera, F.; Pérez-Inestrosa, E.; Álvarez, E.; Lassaletta, J. M.; Fernández, R.; Ros, A.; Pischel, U. *Chem. - Eur. J.* **2015**, *21*, 15369–15376.
- Bachollet, S. P. J. T.; Volz, D.; Fiser, B.; Minch, S.; Röncke, F.; Carrillo, J.; Adams, H.; Schepers, U.; Gómez-Bengo, E.; Bräse, S.; Harrity, J. P. A. *Chem. - Eur. J.* **2016**, *22*, 12430–12438.
- Pais, V. F.; Ramírez-Lopez, P.; Romero-Arenas, A.; Collado, D.; Nájera, F.; Pérez-Inestrosa, E.; Fernández, R.; Lassaletta, J. M.; Ros, A.; Pischel, U. *J. Org. Chem.* **2016**, *81*, 9605–9611.



- (25) Wang, J.; Wu, Q.; Yu, C.; Wei, Y.; Mu, X.; Hao, E.; Jiao, L. *J. Org. Chem.* **2016**, *81*, 11316–11323.
- (26) Lee, B.; Park, B. G.; Cho, W.; Lee, H. Y.; Olsasz, A.; Chen, C.-H.; Park, S. B.; Lee, D. *Chem. - Eur. J.* **2016**, *22*, 17321–17328.
- (27) Patalag, L. J.; Jones, P. G.; Werz, D. B. *Angew. Chem., Int. Ed.* **2016**, *55*, 13340–13344.
- (28) Ibarra-Rodríguez, M.; Muñoz-Flores, B. M.; Dias, H. V. R.; Sánchez, M.; Gomez-Treviño, A.; Santillan, R.; Farfán, N.; Jimenez-Pérez, V. M. *J. Org. Chem.* **2017**, *82*, 2375–2385.
- (29) Lamère, J. F.; Lacroix, P. G.; Farfán, N.; Rivera, J. M.; Santillan, R.; Nakatani, K. *J. Mater. Chem.* **2006**, *16*, 2913–2920.
- (30) Schiller, A.; Wessling, R. A.; Singaram, B. *Angew. Chem., Int. Ed.* **2007**, *46*, 6457–6459.
- (31) Rodríguez, M.; Ramos-Ortiz, G.; Alcalá-Salas, M. I.; Maldonado, J. L.; López-Varela, K. A.; López, Y.; Domínguez, O.; Meneses-Nava, M. A.; Barbosa-García, O.; Santillan, R.; Farfán, N. *Dyes Pigm.* **2010**, *87*, 76–83.
- (32) Kubo, Y.; Nishiyabu, R.; James, T. D. *Chem. Commun.* **2015**, *51*, 2005–2020.
- (33) Flagstad, T.; Petersen, M. T.; Nielsen, T. E. *Angew. Chem., Int. Ed.* **2015**, *54*, 8395–8397.
- (34) Elstner, M.; Weisshart, K.; Müllen, K.; Schiller, A. *J. Am. Chem. Soc.* **2012**, *134*, 8098–8100.
- (35) Santos, F. M. F.; Rosa, J. N.; Candeias, N. R.; Carvalho, C. P.; Matos, A. I.; Ventura, A. E.; Florindo, H. F.; Silva, L. C.; Pischel, U.; Gois, P. M. P. *Chem. - Eur. J.* **2016**, *22*, 1631–1637.
- (36) Cal, P. M. S. D.; Sieglitz, F.; Santos, F. M. F.; Carvalho, C. P.; Guerreiro, A.; Bertoldo, J. B.; Pischel, U.; Gois, P. M. P.; Bernardes, G. J. L. *Chem. Commun.* **2017**, *53*, 368–371.
- (37) Klymchenko, A. S. *Acc. Chem. Res.* **2017**, *50*, 366–375.
- (38) Denk, W.; Strickler, J. H.; Webb, W. W. *Science* **1990**, *248*, 73–76.
- (39) Xu, C.; Webb, W. W. *J. Opt. Soc. Am. B* **1996**, *13*, 481–491.
- (40) Laurent, A. D.; Le Guennic, B.; Jacquemin, D. *Theor. Chem. Acc.* **2016**, *135*, 173.
- (41) McDaniel, D. H.; Brown, H. C. *J. Org. Chem.* **1958**, *23*, 420–427.
- (42) Lippert, E. Z. *Naturforsch., A: Phys. Sci.* **1955**, *10*, 541–545.
- (43) Mataga, N.; Kaifu, Y.; Koizumi, M. *Bull. Chem. Soc. Jpn.* **1955**, *28*, 690–691.
- (44) Mataga, N.; Kaifu, Y.; Koizumi, M. *Bull. Chem. Soc. Jpn.* **1956**, *29*, 465–470.
- (45) Didier, P.; Ulrich, G.; Mély, Y.; Ziessel, R. *Org. Biomol. Chem.* **2009**, *7*, 3639–3642.
- (46) Pawlicki, M.; Collins, H. A.; Denning, R. G.; Anderson, H. L. *Angew. Chem., Int. Ed.* **2009**, *48*, 3244–3266.
- (47) Zhang, X.; Xiao, Y.; Qi, J.; Qu, J.; Kim, B.; Yue, X.; Belfield, K. D. *J. Org. Chem.* **2013**, *78*, 9153–9160.
- (48) Kim, D.; Ryu, H. G.; Ahn, K. H. *Org. Biomol. Chem.* **2014**, *12*, 4550–4566.
- (49) Kim, H. M.; Cho, B. R. *Chem. Rev.* **2015**, *115*, 5014–5055.
- (50) Subedi, P. The Two-Photon Excitation Fluorescence (TPEF) Enhancement of Dipolar Organic Chromophores in Y Zeolites. *M.Sc. Thesis*, Dalhousie University, March 2016.
- (51) Chiba, S.; Zhang, L.; Lee, J.-Y. *J. Am. Chem. Soc.* **2010**, *132*, 7266–7267.
- (52) Weng, J.-Q.; Deng, Q.-M.; Wu, L.; Xu, K.; Wu, H.; Liu, R.-R.; Gao, J.-R.; Jia, Y.-X. *Org. Lett.* **2014**, *16*, 776–779.
- (53) Cho, B. R.; Son, K. H.; Lee, S. H.; Song, Y.-S.; Lee, Y.-K.; Jeon, S.-J.; Choi, J. H.; Lee, H.; Cho, M. *J. Am. Chem. Soc.* **2001**, *123*, 10039–10045.
- (54) Rumi, M.; Perry, J. W. *Adv. Opt. Photonics* **2010**, *2*, 451–518.
- (55) Gu, P.-Y.; Lu, C.-J.; Hu, Z.-J.; Li, N.-J.; Zhao, T.-T.; Xu, Q.-F.; Xu, Q.-H.; Zhang, J.-D.; Lu, J.-M. *J. Mater. Chem. C* **2013**, *1*, 2599–2606.